Published in final edited form as:
Science. 2010 September 24; 329(5999): 1645–1647. doi:10.1126/science.1192046.

Parasympathetic innervation maintains epithelial progenitor cells during salivary organogenesis

S.M. Knox[1], **I.M.A. Lombaert**[1], **X. Reed**[1], **L Vitale-Cross**[2], **J.S. Gutkind**[2], and **M.P. Hoffman**[1,*]
[1]Matrix and Morphogenesis Unit, LCDB,

[2]OPCB, NIDCR, NIH, 30 Convent Dr, Bethesda, MD 20892, USA.

Abstract

The maintenance of a progenitor cell population as a reservoir of undifferentiated cells is required for organ development and regeneration. However, the mechanisms by which epithelial progenitor cells are maintained during organogenesis are poorly understood. We report that removal of the parasympathetic ganglion in mouse explant organ culture decreased the number and morphogenesis of keratin 5-positive epithelial progenitor cells. These effects were rescued with an acetylcholine analog. We demonstrate that acetylcholine signaling, via the muscarinic M1 receptor and EGFR, increased epithelial morphogenesis and proliferation of the keratin 5-positive progenitor cells. Parasympathetic innervation maintained the epithelial progenitor cell population in an undifferentiated state, which was required for organogenesis. This mechanism for epithelial progenitor cell maintenance may be targeted for organ repair or regeneration.

Organogenesis involves the coordinated growth of epithelium, mesenchyme, nerves, and blood vessels, which use common sets of genes, guidance cues, and growth factor signaling pathways (1-5). Research on epithelial organogenesis has focused on epithelial-mesenchymal and endothelial-epithelial cell interactions. However, the function of the peripheral nervous system during epithelial organogenesis is less clear.

Pavlov's seminal experiments on dogs demonstrated that neuronal input controls salivary gland function (6) and, more recent work showed that parasympathetic innervation of salivary glands is essential for regeneration after injury (7). Since parasympathetic innervation occurs in parallel with salivary gland development (8), we hypothesized that parasympatheic innervation is required for epithelial progenitor cell function during organogenesis.

To test this hypothesis, we used mouse embryonic submandibular gland (SMG) explant culture and mechanically removed the parasympathetic submandibular ganglion (PSG) before the gland developed. SMG development begins at embryonic day 11 (E11), when the oral epithelium invaginates into neural crest-derived mesenchyme (9). The neuronal bodies of the PSG condense around the epithelium at E12 (fig S1A) and could be separated from epithelium and mesenchyme in explant culture. When the separated tissues were recombined in culture, the growth of the SMG epithelium was reduced with a significant decrease in the number of end buds in the absence of the PSG (Fig 1A-B, fig S2A). The PSG axons have abundant varicosities (fig S2B, box) that contain the neurotransmitter acetylcholine (ACh) (8), and express the ACh synthetic enzyme (*Chat*) (fig S1B and C). ACh activates epithelial muscarinic (M)-receptors and M1 (*Chrm1*) is the major muscarinic receptor in the embryonic SMG epithelium (fig S1B and C), whereas M1 and M3 (*Chrm3*) stimulate saliva

*Corresponding author: mhoffman@mail.nih.gov.

secretion in the adult (7). Alternatively, we perturbed ACh/M1 signaling using the chemical inhibitors, 4-DAMP (DAMP; N-2-chloroethyl-4-piperidinyl diphenylacetate), an irreversible M1/M3 inhibitor (Fig 1C), atropine, a competitive muscarinic antagonist (fig S2D), beta-bungarotoxin (Btx), which depletes neuronal ACh stores (fig S2E), and siRNA to M1 (*Chrm1*) (fig S2H-I). All treatments reduced the number of end buds (fig S2C-I). In contrast, inhibition of alpha-2 adrenergic receptors with idazoxan had no effect (fig S2F). These experiments demonstrate that epithelial morphogenesis requires PSG, ACh, and M1 activity.

Epithelial morphogenesis may also depend on the size of the epithelial progenitor pool and growth factor-mediated proliferation (10). To distinguish between these two possibilities, we measured expression of epithelial progenitor markers and growth factor signaling pathways present during SMG development. We found that removal of the PSG reduced gene expression of the epithelial progenitor cell markers cytokeratins-5 (*Krt5*) and −15 (*Krt15*), as well as aquaporin 3 (*Aqp3*) (Fig 1D), and did not affect genes involved in FGF and EGF signaling. Cytokeratin-5 protein (referred to as K5) is a basal epithelial cell marker in adult salivary glands (11-13). Developing SMGs contain 9.6 ± 1.3% of K5+ cells by FACS analysis, which are present in the end buds and ducts (fig S3A-C). K5+ cells are progenitor cells in the trachea (14) and prostate (15) and we confirmed that they are progenitor cells in the SMG by lineage tracing analysis (fig S3D-H). Cytokeratin-15 protein (K15) can physically pair with K5 (16); and Aqp3 is an epithelial progenitor cell marker in the lung (14, 17). *Krt5, Krt15*, and *Aqp3* were downregulated in intact SMGs after only 4 hours of DAMP treatment (Fig 1D), indicating that they are regulated by ACh/M1 signaling. Taken together, these data support our hypothesis that the PSG neurons modulate epithelial morphogenesis by affecting epithelial progenitor cells via ACh/M1 signaling.

To investigate how ACh directly influences the epithelium, we cultured isolated SMG epithelia in a 3D extracellular matrix with FGF10 (18). We hypothesized that carbachol (CCh), an ACh analog, would increase epithelial morphogenesis and proliferation by increasing the K5+ progenitor cell population. Since ACh/M1 signaling transactivates EGFR by MMP-mediated release of HBEGF in prostate epithelium (19), we predicted that 1) HBEGF would increase K5+ cell proliferation, and 2) an EGFR antagonist (PD168393 referred to here as PD) would inhibit CCh-induced K5+ cell proliferation. As expected, CCh and HBEGF increased epithelial morphogenesis, proliferation, and K5 staining, in an EGFR-dependent manner (Fig 2A-F; fig S4A-B). Furthermore, CCh increased EGFR protein expression (fig S4C-F), and CCh-mediated morphogenesis was inhibited by PD (fig S4G), suggesting that muscarinic-induced morphogenesis required endogenous EGFR activity. When CCh and HBEGF were combined, they had a greater-than-additive effect on morphogenesis and proliferation, which were both inhibited by PD (Fig 2D-F). However, the combination did not have an additive effect on K5 staining. Therefore, CCh and HBEGF operate in the same pathway to maintain K5, and they increase proliferation of cells that do not express K5.

To investigate this further, we analyzed differentiation of the K5+ cell population. K5+ progenitor cell differentiation occurs in a similar manner to that described for the prostate (15); as the basal K5+K19- progenitor cells differentiate towards the developing lumen, they co-express K19 (K5+K19+), and as differentiation proceeds, they lose K5 (K5-K19+) (Fig 2G; fig S5). Thus, the K5+ cell population (Fig 2A-F) includes both basal K5+K19- cells and K5+K19+ cells. To identify differences in the response to either CCh or HBEGF, we counted the proliferating cells (EdU+) that were K5+K19- (green), K5+K19+ (yellow), or K5-K19+ (red) (Fig 2H and fig S5). An important finding was that CCh doubled the percentage of proliferating basal K5+K19- progenitor cells from 20 to 40 % of the EdU+ cells. CCh also increased K5+K19+ cell proliferation, suggesting that these cells are still responsive to muscarinic activation. HBEGF increased the proliferation of both the

K5+K19+ and K5-K19+ cells, suggesting that HBEGF promotes differentiation along the K19+ lineage. The combination of CCh and HBEGF resulted in similar amounts of proliferation of K5+K19-, K5+K19+, and K5-K19+ cells (Fig 2F). Finally, CCh- and HBEGF-mediated proliferation of the K5+ and K19+ cells was completely inhibited by PD (Fig 2H) although proliferating cells that were not K5+ or K19+ were still present (Fig 2F). Taken together, these data suggest that CCh/M1 signaling maintains the K5+ progenitor cell population in an EGFR-dependent manner, and that HBEGF/EGFR increases differentiation of the K19+ cell lineage.

We confirmed these findings in the intact SMG, by using a loss-of-function approach, treating SMGs with DAMP or PD. We hypothesized that DAMP treatment would inhibit K5+ cell proliferation and result in fewer K5+ cells. We used fluorescence-activated cell sorting (FACS) analysis of the E-cadherin+ epithelial population, measuring the number of cells expressing K5, K19, and Ki67, for proliferating cells (fig S6A-D). As expected, the total K5+ cell population was reduced by both DAMP and PD treatment. The reduction in K5+ cell number was not due to an increase in apoptosis (fig S7). Importantly, both PD and DAMP, completely inhibit proliferation of the K5+K19- basal progenitor cells. In sum, the inhibition of M1 and EGFR signaling in the intact SMG reduces the number of K5+K19- progenitor cells by inhibiting their proliferation. These data demonstrate that the maintenance of K5+ cells in an undifferentiated state (K5+K19-) in the intact SMG is dependent on M1 and EGFR signaling.

These findings suggest that K5+ progenitor cells express both M1 and EGFR. Using immunostaining and FACS analysis we demonstrated that the majority of K5+ cells (68 %) expressed both EGFR and M1 (fig S8A-H), suggesting that the effects of CCh and HBEGF are cell-autonomous. Furthermore, the combination of HBEGF and CCh increased the amount of both M1 and EGFR in the epithelium (fig S8J-N), demonstrating that positive feedback increases receptor expression.

We then predicted that CCh would rescue epithelial morphogenesis and K5 expression in the PSG-free SMG explants in an EGFR-dependent manner. As expected, treatment of SMG with PD, or removal of the PSG, decreased the number of end buds and K5 staining compared to control (Fig 3A-E; fig S9). Treatment of the PSG-free explants with CCh increased the number of end buds and K5 expression, which were inhibited by PD (Fig 3C-E). Furthermore, PD reduced K19 expression in the absence of the PSG, demonstrating that endogenous HBEGF maintains the K19+ cells. HBEGF increases SMG morphogenesis by inducing MT2-MMP and FGFR expression (20). Thus, addition of PD to PSG-free explants reduces the EGFR-dependent morphogenesis, and the remaining growth is likely FGFR2b-dependent (9, 18).

Our data demonstrate that parasympathetic innervation maintains K5+ progenitor cells during epithelial organogenesis. A therapeutic implication is that postnatal epithelial regeneration of salivary glands may require muscarinic stimulation of the K5+ progenitor cells. Indeed, culture of denervated lobules of adult SMGs with CCh increased K5 and *Krt5* expression, which were both reduced with DAMP+PD (Fig 4A-D, fig S10A). In addition, K5+ cells increase during regeneration of adult SMGs after duct ligation when the innervation to the gland is intact (21). Furthermore, other organs that contain K5+ progenitor cells, such as the prostate (15), the skin and its appendages (22), the airway epithelium and trachea (14), and taste buds (23), are innervated by the peripheral parasympathetic nervous system (24) during development. We analyzed the developing ventral prostate of P6 mice, which contain basal K5 cells and innervation from the pelvic ganglion neurons (fig S10B). The addition of DAMP+PD to prostate organ culture also decreased K5 expression (Fig 4E-F, fig S10C)), and reduced *Krt5, Krt14*, and *Aqp3* (Fig 4G). Thus, we report a mechanism

by which K5+ epithelial progenitor cells are maintained during development, which has implications for understanding how tissue-specific epithelial progenitor cells could be targeted for organ repair or regeneration.

Supplementary Material

Refer to Web version on PubMed Central for supplementary material.

Acknowledgments

The authors would like to thank V. N. Patel, I. T. Rebustini, L. M. Angerer, K. G. Ten-Hagen, K. M. Yamada, and S. Powers for discussions and critical reading of this manuscript. The study was supported by the Intramural Research Program of the NIDCR, NIH.

References

1. Lu P, Werb Z. Science. Dec 5.2008 322:1506. [PubMed: 19056977]
2. Hogan BL. Cell. Jan 22.1999 96:225. [PubMed: 9988217]
3. Matsumoto K, Yoshitomi H, Rossant J, Zaret KS. Science. Oct 19.2001 294:559. [PubMed: 11577199]
4. Lammert E, Cleaver O, Melton D. Science. Oct 19.2001 294:564. [PubMed: 11577200]
5. Carmeliet P, Tessier-Lavigne M. Nature. Jul 14.2005 436:193. [PubMed: 16015319]
6. Pavlov IP. Science. 1906; 24:613. [PubMed: 17771162]
7. Proctor GB, Carpenter GH. Auton Neurosci. Apr 30.2007 133:3. [PubMed: 17157080]
8. Coughlin MD. Dev Biol. Mar.1975 43:123. [PubMed: 1149921]
9. Patel VN, Rebustini IT, Hoffman MP. Differentiation. Sep.2006 74:349. [PubMed: 16916374]
10. Stanger BZ, Tanaka AJ, Melton DA. Nature. Feb 22.2007 445:886. [PubMed: 17259975]
11. Raimondi AR, Vitale-Cross L, Amornphimoltham P, Gutkind JS, Molinolo A. Am J Pathol. May. 2006 168:1654. [PubMed: 16651631]
12. Macias E, de Marval PL, Senderowicz A, Cullen J, Rodriguez-Puebla ML. Cancer Res. Jan 1.2008 68:162. [PubMed: 18172308]
13. Vitale-Cross L, Amornphimoltham P, Fisher G, Molinolo AA, Gutkind JS. Cancer Res. Dec 15.2004 64:8804. [PubMed: 15604235]
14. Rock JR, et al. Proc Natl Acad Sci U S A. Aug 4.2009 106:12771. [PubMed: 19625615]
15. Hudson DL, et al. J Histochem Cytochem. Feb.2001 49:271. [PubMed: 11156695]
16. Peters B, Kirfel J, Bussow H, Vidal M, Magin TM. Mol Biol Cell. Jun.2001 12:1775. [PubMed: 11408584]
17. Avril-Delplanque A, et al. Stem Cells. Aug.2005 23:992. [PubMed: 16043462]
18. Steinberg Z, et al. Development. Mar.2005 132:1223. [PubMed: 15716343]
19. Prenzel N, et al. Nature. Dec 23-30.1999 402:884. [PubMed: 10622253]
20. Rebustini IT, et al. Dev Cell. Oct.2009 17:482. [PubMed: 19853562]
21. Hai B, et al. Stem Cells Dev. Mar 30.2010
22. Blanpain C, Fuchs E. Nat Rev Mol Cell Biol. Mar.2009 10:207. [PubMed: 19209183]
23. Okubo T, Clark C, Hogan BL. Stem Cells. Feb.2009 27:442. [PubMed: 19038788]
24. Schafer MK, Eiden LE, Weihe E. Neuroscience. May.1998 84:361. [PubMed: 9539210]

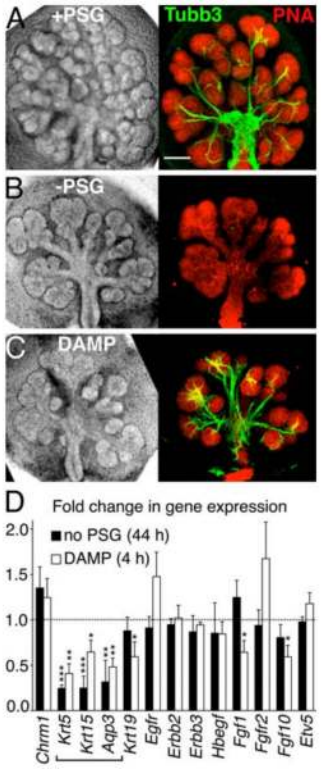

Fig 1. Removal of the PSG in mouse SMG explant culture decreases branching morphogenesis and expression of basal progenitor cell markers

SMGs were cultured for 44 hrs with (**A**) or without (**B**) the PSG or treated with a muscarinic inhibitor (DAMP) (**C**). Whole-mount images of the nerves (beta-3 tubulin, Tubb3) and the epithelium (peanut agglutinin, PNA) are shown. Scale bar = 200 μm. (**D**) qPCR analysis of gene expression. Mean ± SEM of three experiments. Students t-test; $*P < 0.05$, $**P < 0.01$, $***P < 0.001$.

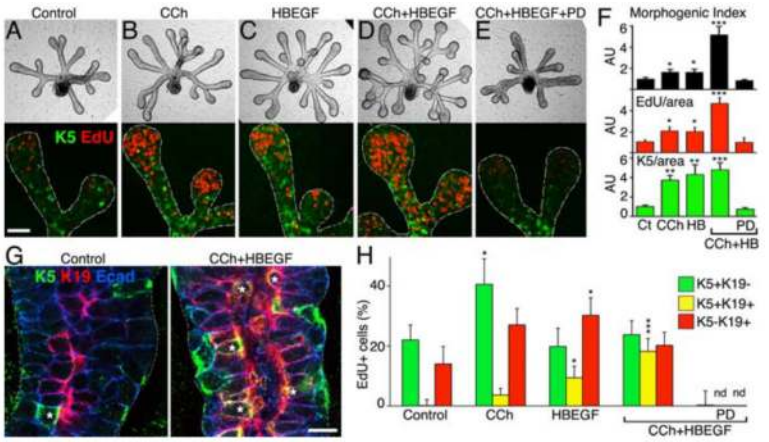

Fig 2. Activation of muscarinic receptors maintains K5+K19- progenitor cells in an EGFR-dependent manner

Epithelia were cultured in control media (**A**), with CCh (**B**), HBEGF (**C**), CCh+HBEGF (**D**), CCh+HBEGF+PD (**E**). Immunostaining of proliferation (EdU) and K5+ cells is shown. Images are 3 μM confocal sections; scale bar = 50 μm. (**F**) Quantification of epithelial morphogenesis, proliferation, and K5 protein. AU = arbitrary units × 100. (**G**) Epithelia were immunostained for K5 and K19. Yellow cells expressing both K5 and K19 are marked by white*. Images are 2 μM confocal sections; scale bar = 10 μm. (**H**) Quantification of the number of proliferating cells; see fig S5 for images. Mean ± SEM of three experiments. ANOVA with post hoc Dunnetts test; $*P < 0.05$, $**P < 0.01$, $***P < 0.001$.

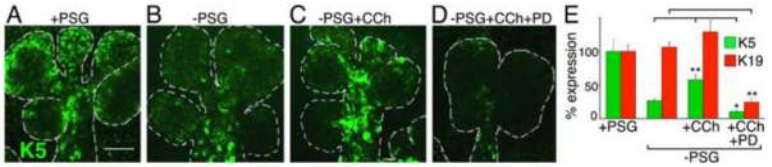

Fig 3. CCh rescues branching morphogenesis and K5+ progenitor cells in an EGFR-dependent manner

SMG explants, recombined with (**A**) or without (**B-D**) the PSG, were cultured with CCh (**C**) or CCh+PD (**D**). Images are single confocal sections (2 μM); scale bar = 50 μm (**E**) Quantification of K5 and K19 fluorescence. Mean ± SEM of three experiments. ANOVA with post hoc Dunnetts test; $*P < 0.05$, $**P < 0.01$.

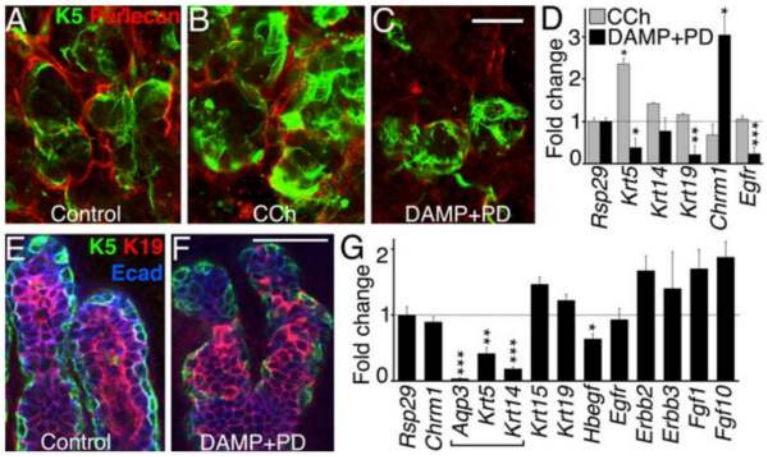

Fig 4. Muscarinic receptor/EGFR signaling controls K5+ progenitor cell maintenance in the adult SMG and developing prostate

Denervated adult SMGs (**A**) cultured with CCh (**B**) or DAMP+PD (**C**), were immunostained for K5 and perlecan, and analyzed by qPCR (**D**). Scale bar = 20 μm, see fig S10 for quantification. Ventral prostates from P6 mice (**E**) were cultured ± DAMP+PD (**F**) and stained for K5, K19 and E-cadherin, and gene expression was analyzed by qPCR (**G**). Scale bars = 50 μm. Mean ± SEM of three experiments. Students t-test; **P* < *0.05*, ***P* < *0.01*, ****P* < *0.001*.